 DOI: 10.1086/662670

Appendix B from N. Mideo et al., "Causes of Variation in Malaria Infection Dynamics: Insights from Theory and Data"

(Am. Nat., vol. 178, no. 6, p. 174)

Supplementary Results

Statistical Analyses of Experimental Data

Tables B1 and B2 present statistics from linear mixed effects models of invasion rate variation and linear models of burst size variation. Histograms showing the burst size observations across treatment groups are shown in figure B1.

Assessing Model "Goodness of Fit"

We compare the fit of our original model (Mideo et al. 2008*b*) with that of the hybrid model, which includes multiple forms of immunity, by plotting the overlaid standardized residuals for parasite and RBC densities for each model (fig. B2). When the mean of the standardized residuals lies outside the 95% (Bonferroni corrected for multiple tests) predictive interval (i.e., the red line falls outside of the dashed lines), this suggests that the model is over- or underestimating the data, and is suggestive of a poor fit. While there are clearly some time points for which neither model captures the data well, overall the hybrid model is fitting better (fig. B2, *right*). The early time points for which the RBC densities are fitted poorly is not particularly surprising since there is a lot of unexplained variation in the data at these very early days postinfection.

Model Inferences

The most likely model includes immune responses that independently target merozoites, parasitized RBCs, and unparasitized RBCs, although not every response is necessary to explain the dynamics of every individual mouse. This individual variation is evident in the posterior predictive intervals for the different immune responses, depicted below (figs. B3–B5). Overall, immune responses targeting merozoites and parasitized RBCs are more important for explaining the dynamics of infections with the more virulent clone AS than with the less virulent clone DK. The marginal posterior distributions for all other parameters are given in figure B6.

Refitting Original Data

Given that the model we presented in Mideo et al. (2008*b*) was assessed as providing a "good fit" to the data used in that study, we refit that data (originally from Barclay et al. 2008) to the Mideo et al. (2008*b*) model and the Miller et al. (2010) model using the Bayesian framework of this study. As with the new data we explore in the main text, the immune response is necessary to explain the data from infections with the more virulent genotype, but not the avirulent genotype (table B3).

In figure B6, we compare the best fits from Mideo et al. (2008*b*), where models were fitted only to parasite data, with the new hybrid model fitted to this same data.

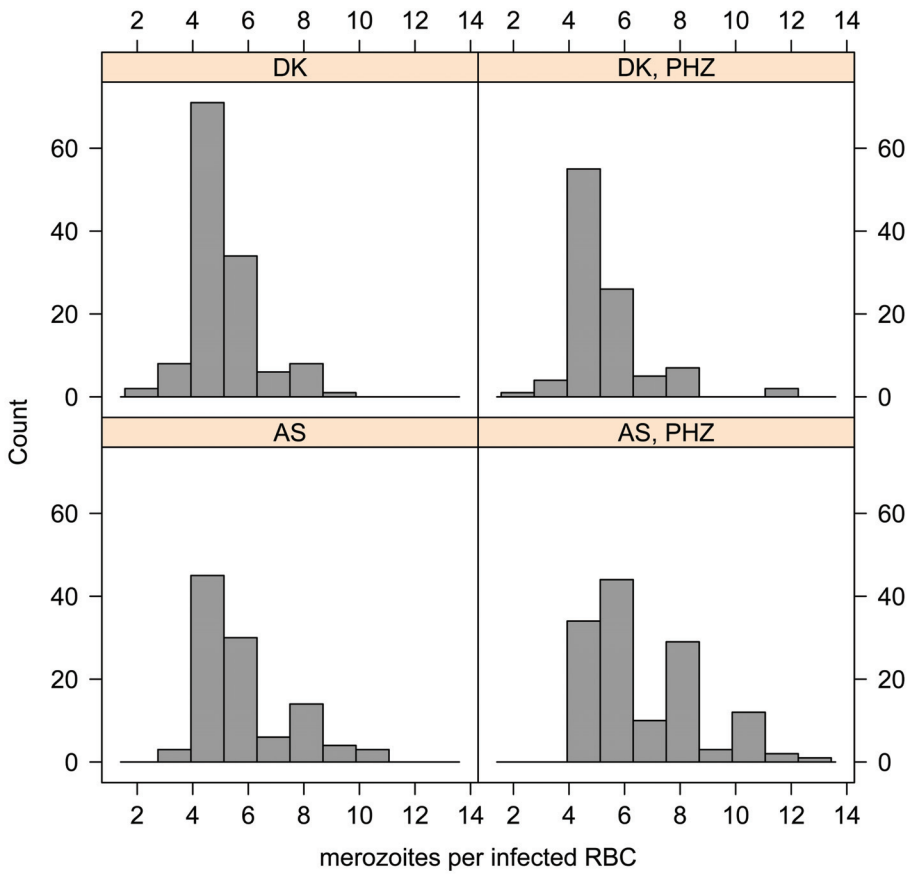

Figure B1: Histogram of burst size observations across treatments. Burst sizes were estimated by counting the number of merozoites in at least 25 mature schizonts for each individual infected mouse. The distributions here are plotted from pooling this data according to the genotype of the infecting parasites (DK or AS) and phenylhydrazine treatment (PHZ or none).

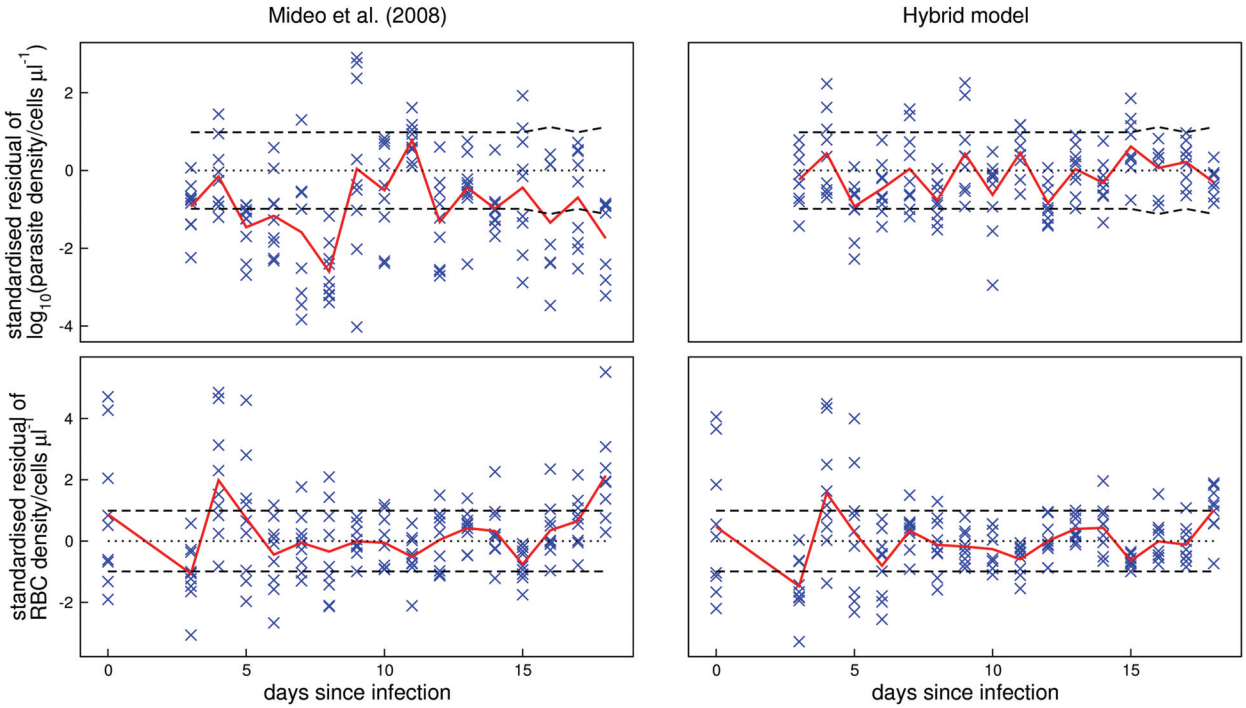

Figure B2: Standardized residuals of the fit of the age-structured model of Mideo et al. (2008*b*; *left*) and the fit to the hybrid model (*right*) to newly collected data. *Top*, Parasite density; *bottom*, red blood cell density. Each cross represents the standardized residual on a particular day for an individual mouse. The red line joins the means of the standardized residuals for each day, and the dashed lines denote the 95% (Bonferroni corrected for multiple tests) predictive intervals of the mean standardized residual assuming the model is true. The *Y*-axis is scaled to units of standard deviations.

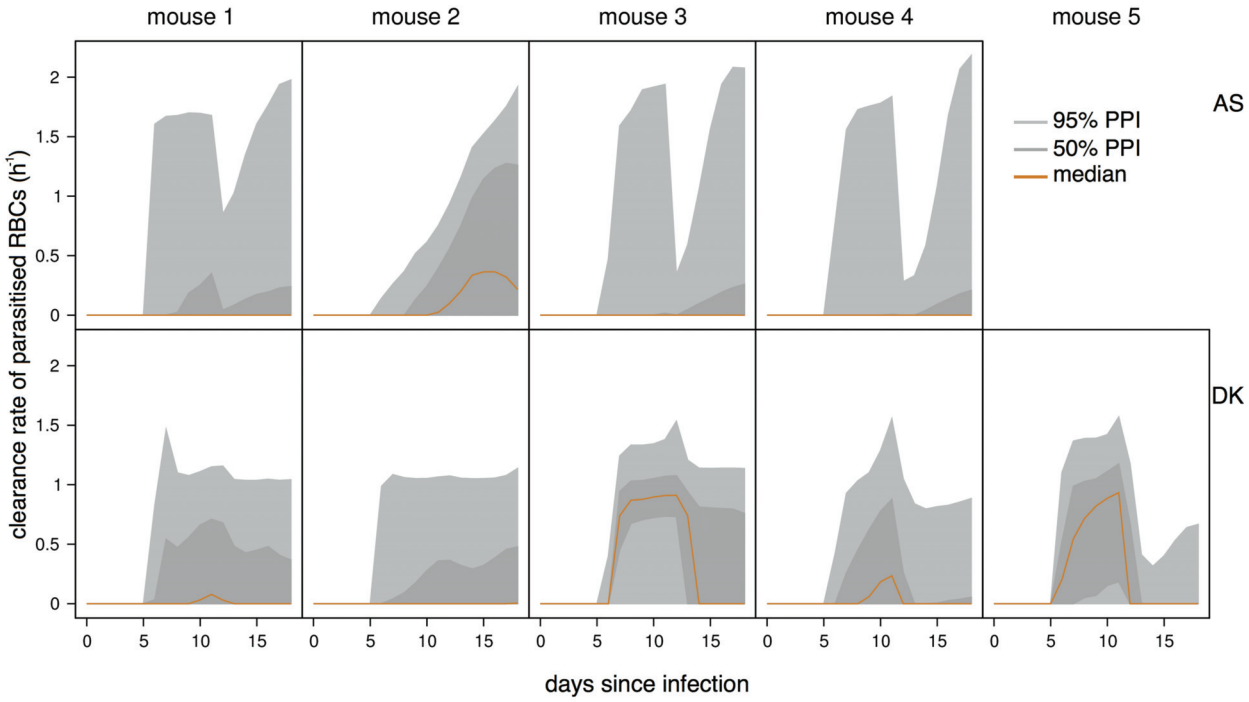

Figure B3: Posterior predictive interval (PPI) of immune responses targeting parasitized red blood cells (RBCs). Solid lines give best-fit function describing clearance rate. Light gray regions correspond to 95% PPI; dark gray regions correspond to 50% PPI.

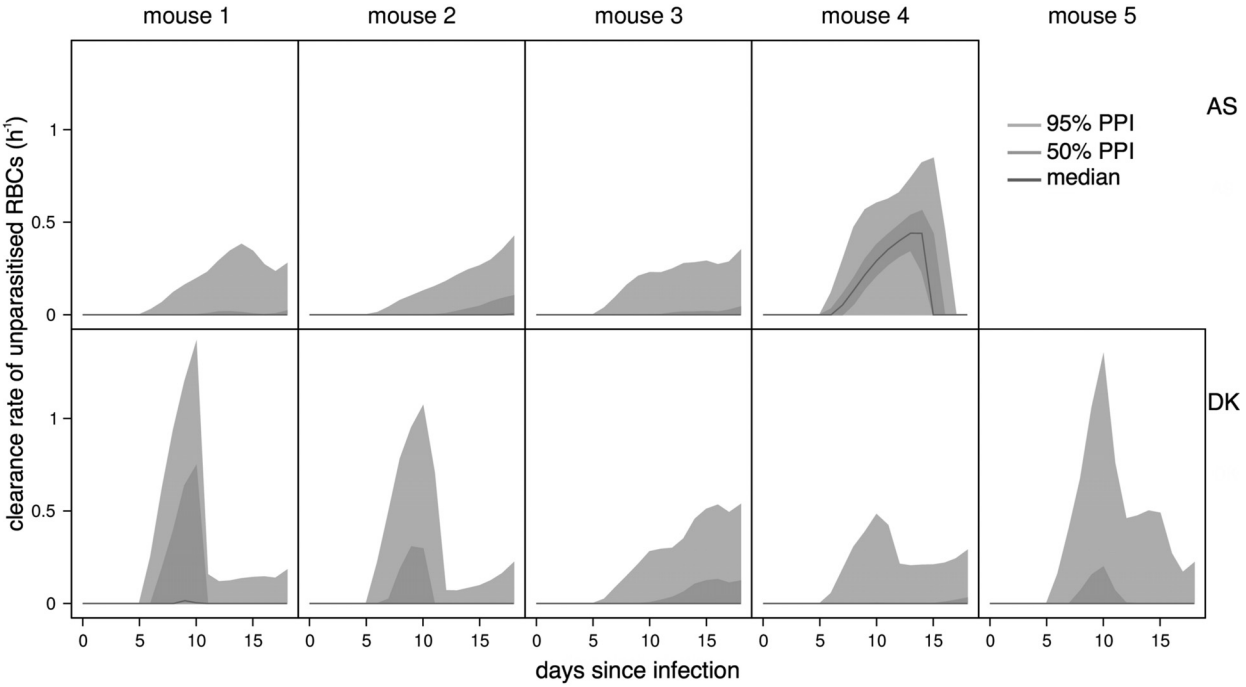

Figure B4: Posterior predictive interval (PPI) of immune responses targeting unparasitized red blood cells (RBCs; i.e., bystander death). Solid lines give best-fit function describing clearance rate. Light gray regions correspond to 95% PPI; dark gray regions correspond to 50% PPI.

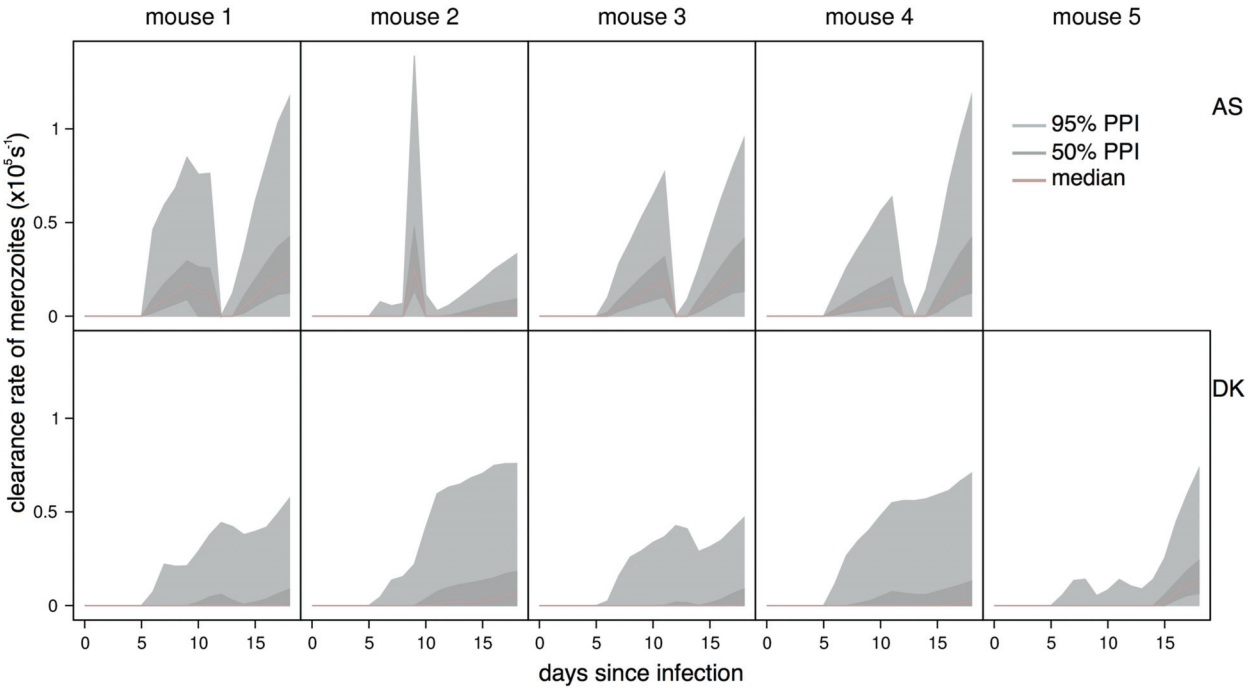

Figure B5: Posterior predictive interval (PPI) of immune responses targeting merozoites. Solid lines give best-fit function describing total clearance. Light gray regions correspond to 95% PPI; dark gray regions correspond to 50% PPI.

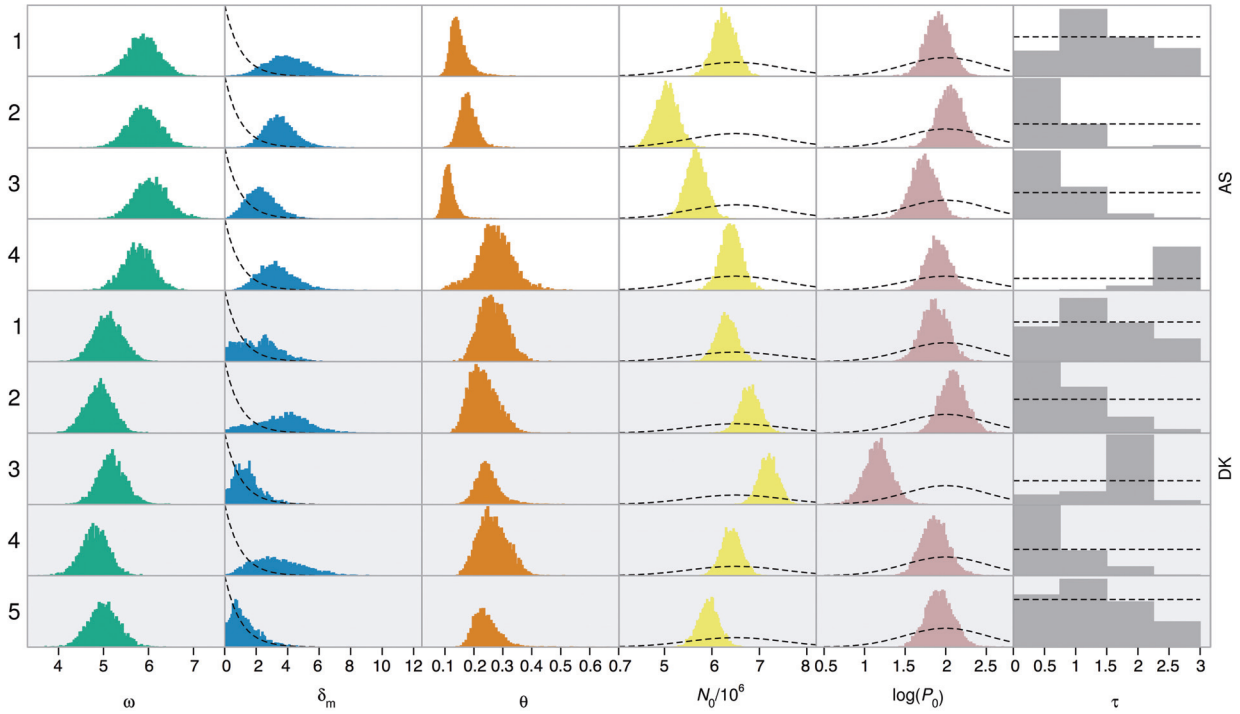

Figure B6: Marginal distributions of fitted parameters for the most likely reduced hybrid model. Each row corresponds to an individual mouse. White panels are for individuals infected with the more virulent genotype AS; gray panels are for individuals infected with the less virulent genotype DK. Dashed lines indicate the prior distributions on each parameter. Units are given in table A1.

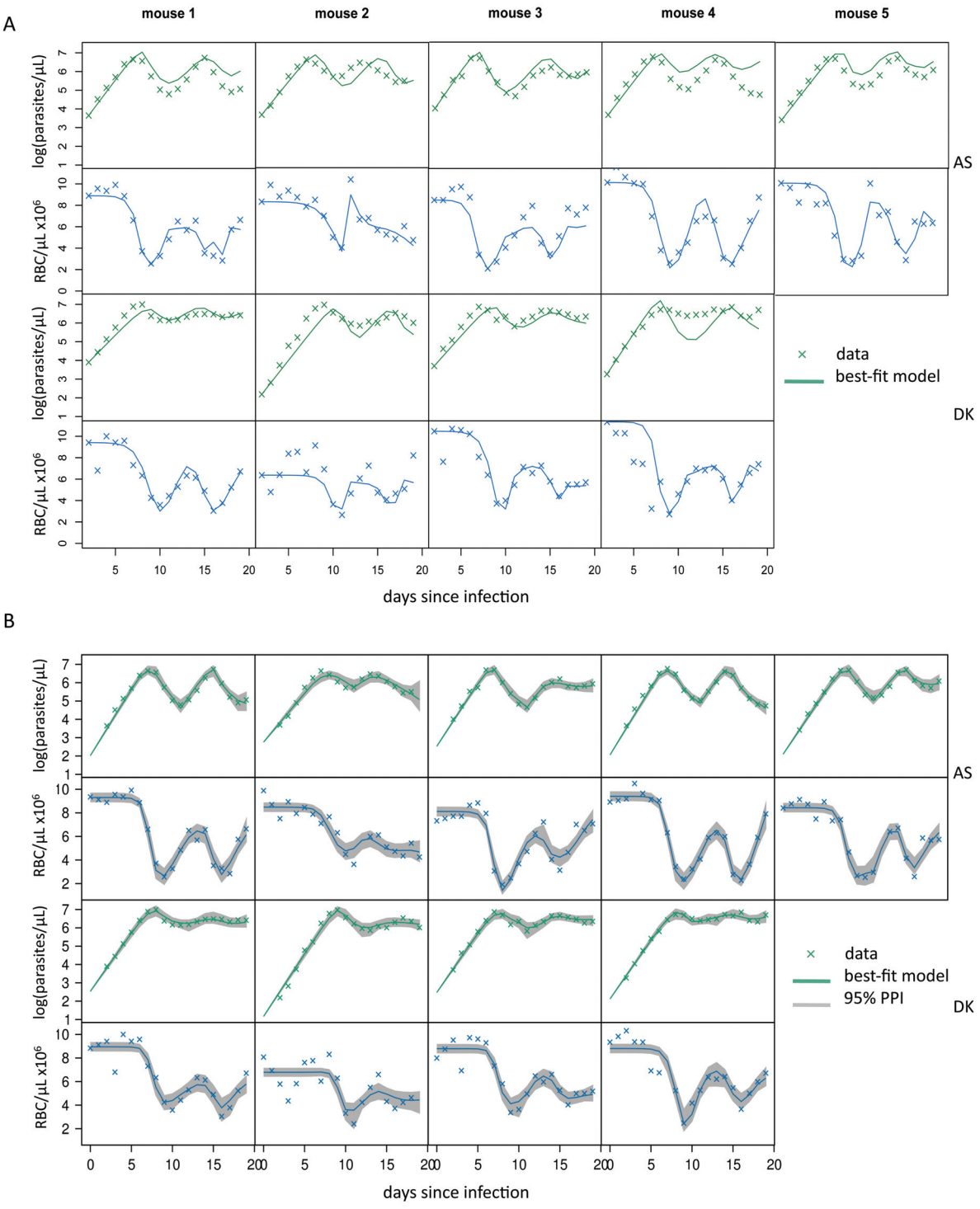

Figure B7: Comparison of model fits. *A*, Original best fit of red blood cell (RBC) age-structured model with no immunity, fitted to data from Barclay et al. (2008). Redrawn from Mideo et al. (2008*b*). *B*, Fit of hybrid model (including RBC age-structure and immune responses) to the same data set.

Table B1. Analysis of red blood cell (RBC) invasion rates in $CD4^+$-depleted mice

	LRT (χ^2)	*P*
Minimal model:		
RBC age	NA	
Genotype	NA	
Genotype : RBC age	$\chi^2_1 = 8.234$	.004
Nonsignificant terms deleted from maximal model:		
Mass of mouse	$\chi^2_1 = .380$	.538

Note: LRT = likelihood ratio test; NA = not applicable.

Table B2. Analysis of burst sizes in $CD4^+$-depleted mice

	F	*P*
Minimal model:		
Genotype	$F_{1,15} = 11.021$	.005
Phenylhydrazine	$F_{1,15} = 4.067$	.062
Nonsignificant terms deleted from maximal model:		
Mass of mouse	$F_{1,14} = .893$	.361
Parasite density	$F_{1,13} = .181$	.677
Uninfected red blood cell density	$F_{1,12} = .317$	.584
Genotype : phenylhydrazine	$F_{1,11} = .975$	.345

Table B3. Comparing the fit of original model from Mideo et al. (2008*b*) with the Miller et al. (2010) model of the main text using Bayes factors (BFs)

Genotype	BF	Interpretation of BF
AS	1.1×10^{40}	AS data are overwhelming more likely under the Miller et al. (2010) model
DK	4.5×10^{-6}	DK data are overwhelmingly more likely under the Mideo et al. (2008*b*) model, suggesting that the Miller et al. (2010) model overfits the data
All	4.9×10^{36}	Conclusions are the same as those for the newly collected data: immune responses are important for explaining dynamics of more virulent (AS) but not for the less virulent (DK) genotype